

**Qualification of a Medium Current Ion Implantation System in a
Semiconductor Production Environment**

by

Sandra K. Joung

S.B. Materials Science and Engineering
Massachusetts Institute of Technology
(1995)

Submitted to the Department of Materials Science and Engineering
in Partial Fulfillment of the Requirement for the Degree of

MASTER OF SCIENCE IN MATERIALS SCIENCE AND ENGINEERING

at the
Massachusetts Institute of Technology
June 1996

© 1996 Sandra K. Joung. All rights reserved.

The author hereby grants to MIT permission to reproduce and to distribute publicly paper
and electronic copies of this thesis document in whole or in part.

Signature of Author

Department of Materials Science and Engineering
May 10, 1996

Certified by.....

Lionel G. Kimerling
Thomas Lord Professor of Materials Science and Engineering
Thesis Supervisor

Accepted by.....

Michael F. Rubner
TDK Professor of Materials Science and Engineering
Chair, Departmental Committee on Graduate Students

MASSACHUSETTS INSTITUTE
OF TECHNOLOGY

JUN 24 1996 Science

LIBRARIES

Qualification of a Medium Current Ion Implantation System in a Semiconductor Production Environment

by

Sandra K. Joung

Submitted to the Department of Materials Science and Engineering on May 10, 1996 in partial fulfillment of the requirements for the Degree of Master of Science in Materials Science and Engineering

ABSTRACT

A study of the process performance of Eaton NV-8200P medium current ion implanter was conducted during the start up of Motorola's MOS-13 wafer fabrication facility. The implanter was evaluated in order to characterize its baseline performance and verify its qualification for use in an advanced technology, high volume semiconductor production environment. The evaluation included a source inspection test at the Eaton manufacturing facility, a pre-production qualification test, and the Motorola 2.0 Qualification test.

The implanter was accepted at the source inspection and approved for running the first line of production qualification wafer lots. Based on the study results the implanter did not pass the 2.0 qualification test. Several key process performance requirements including dose uniformity, dose repeatability, and metals contamination, did not meet the minimum specifications.

Thesis Supervisor: Dr. Lionel C. Kimerling

Title: Thomas Lord Professor of Materials Science and Engineering

Acknowledgements

There are many people to thank for their contributions to my thesis project. First I'd like to thank Mr. Terry Breeden, my mentor at Motorola, and my MIT thesis advisor, Prof. Lionel Kimerling. Mr. Breeden taught me much of the information I know about ion implantation and was always a fantastic resource of scientific knowledge. I couldn't have accomplished as much as I did at Motorola without his help. I would also like to acknowledge the MOS-13 Implant Team. Thank you for your diligence, patience, and support, during the factory start-up. Your previous experience in the implant area and manufacturing was invaluable to the success of the aggressive implant area start-up. Thanks for your hard work and commitment to the team to meet testing and production deadlines. I would like to acknowledge the Eaton contributions to the start-up effort. The Eaton final test engineers and factory support team headed by Dave Perkins, Jack Hemmer, and Robert Rathmell, were also a wealth of knowledge and provided much support in understanding the fundamental equipment issues. The efforts of the Eaton Field Service Team to implement all the necessary equipment modifications and keeping the tool up for production was greatly appreciated. I'd also like to thank my managers at Motorola, Mr. Rick McFarland and Navjot Chhabra for giving me the co-op experience of a lifetime. It was a thrill being part of the MOS-13 start-up team!

Table of Contents

Chapter 1	Introduction	7
	1.1 Project Motivation.	7
	1.2 Project Objectives	8
	1.3 Thesis Organization	9
Chapter 2	Background	10
	2.1 Introduction.	10
	2.1.1 MOSFET Background	10
	2.1.3 Semiconductor Fabrication	13
	2.2 Ion Implantation Process Theory Background.	15
	2.3 Applications in CMOS Processing.	18
	2.4 Process Requirements and Issues	21
	2.5 Metrology	23
	2.5.1 Therma-wave Thermaprobe Theory	23
	2.5.2 Four Point Probe Theory	25
Chapter 3	Ion Implantation Systems	25
	3.1 Ion Implantation System Theory of Operation	25
	3.2 Eaton NV-8200P Medium Current Ion Implanter	27
Chapter 4	Source Inspection	30
	4.1 Test Description and Procedure.	30
	4.2 Results	32
	4.3 Discussion	33
	4.4 Conclusion	33
Chapter 5	Testing for the RFW Qualification	35
	5.1 Test Description and Procedure.	35
	5.2 Results	36
	5.3 Discussion	37
	5.4 Conclusion	38
Chapter 6	Testing for the 2.0 Qualification	39
	6.1 Test Description and Procedure.	39
	6.2 Results	41
	6.3 Discussion	41
	6.4 Conclusion	44
Chapter 7	Summary	45
Appendix	Statistical Process Control	47
References.	50

List of Figures

Figure 2.1	Schematic of an n-channel MOSFET under standard biasing conditions	11
Figure 2.2	I_{DS} vs V_{GS} for PMOS and NMOS enhancement and depletion mode devices	12
Figure 2.3	Basic process flow for CMOS device fabrication	13
Figure 2.4	Schematic of the range R , projected range R_p , ΔR_p and ΔR_j	14
Figure 2.5	Boron implantation atom distributions for measured data, Pearson IV and Gaussian distributions	16
Figure 2.6	Disorder produced by light ion, heavy ion, and beam of ions forming an amorphous region	16
Figure 2.7	Regions implanted in a standard CMOS process	17
Figure 2.8	Particulate contamination blocking an implant and serving as an elemental contamination source.	20
Figure 2.9	Thermprobe optical system	22
Figure 2.10	Resistivity vs. dopant concentration.	23
Figure 2.11	(a) Linear and (b) square configurations of probe head assemblies	24
Figure 3.1	(a) Freeman source and (b) Bernas source configurations	26
Figure 3.2	Schematic of the NV-8200P Layout	27
Figure 4.1	Beam current glitch.	31
Figure A.1	The normal (Gaussian) distribution.	48
Figure A.2	Control chart.	49

List of Tables

Table 5.1 Process Recipe Matching Data.	37
Table 6.1 Maximum Beam Current Specifications.	40

Chapter 1

Introduction

1.1 Project Motivation

The increasing demand for microcontroller and microprocessor chips continues to fuel the tremendous growth of the semiconductor industry. In order to support the growing demand companies have invested billions of dollars to build new wafer fabrication manufacturing facilities (FABs). The first major milestone for a new manufacturing facility is the factory startup. A FAB startup is one of the most exciting times in the semiconductor industry for both the equipment suppliers and the chip manufacturers. State of the art equipment is purchased and implemented into aggressive manufacturing environments to produce the most advanced products.

During the FAB startup, all of the new process and support equipment is purchased, inspected, installed, and qualified in the shortest amount of time possible. Because of the high risk and cost of misprocessing product wafers (potential revenue), new process equipment must be properly installed and qualified before production can begin. The equipment process quality and production efficiency must be characterized. The heavy demands of process equipment in a manufacturing environment requires production worthy equipment to provide availability (high throughput), reliability, and maintainability. The tool must also prove to be capable of a stable, repeatable process, and the engineer must have the capability to monitor and control that process. After the implanter is qualified it must also be monitored regularly to reduce the risk of misprocessing or damaging product wafers. The FAB startup is critical to the success of the subsequent ramp to full

production. Due to the multimillion dollar cost of ion implanters, one of a kind tools support the product line until additional tools needed to support aggressive throughput schedules can be purchased, installed, and qualified. The pressure to keep the one tool production ready is tremendous because the entire production line will come to a halt if a piece of equipment is not ready or experiencing problems when wafers are scheduled to be processed. The work described in this thesis supported the startup of MOS-13, one of Motorola's new PowerPC manufacturing facilities in Austin, Texas.

1.2 Project Objectives

The project goal was to successfully start up the medium current ion implantation process for production. This included qualifying the medium current implanter, organizing the team of manufacturing operators, equipment maintenance technicians, and engineers who would support the all of the implant processes, and implementing a process-production control system. The implanter qualification required an inspection of the tool at the vendor site, documentation of the baseline performance of the equipment at the Motorola factory site, and verification that the implanter met performance specifications agreed upon in the Motorola Equipment Purchase Agreement (EPA). The performance specifications were outlined in section 2.0 of the EPA. The first medium current implanter was needed for production by September 25, 1995. This thesis describes the methodology of qualifying a medium current ion implanter in a semiconductor production environment.

1.3 Thesis Organization

Chapter 2 reviews the relevant background information. A brief introduction to the semiconductor industry is followed by a discussion of ion implantation theory and its application in CMOS device fabrication.

Chapter 3 discusses the theory of operation of ion implantation systems, including the Eaton NV-8200P medium current ion implanter.

Chapter 4 presents the source inspection methods used to examine 2 NV-8200P medium current ion implantation systems at the manufacturer's factory.

Chapter 5 describes the test procedures and results of the first phase of the system qualification process after the installation at the Motorola site, the pre-production ready for wafers (RFW) qualification.

Chapter 6 reviews the test and results of the complete system 2.0 qualification testing. This qualification verifies that the system meets all of the requirements of the equipment purchase agreement (EPA) as specified in section 2.0.

Chapter 7 summarizes the findings of the work and offers recommendations for future work.

Chapter 2

Background

2.1 Introduction

The growth of the semiconductor market and the continued rapid development of solid state devices are fueled by their numerous applications in the communication, information, computing, and commodity fields. The 10% annual growth of this multibillion dollar industry which drives the electronics industry projects the market to be worth \$112 billion by 1998 [1]. The industry began when Bell Lab's invention of the solid state transistor was thrust into production in the 1950's. Since then, improved technologies have emerged to mass produce transistors on a silicon substrate and shrink device structures to sub-micrometer dimensions. Metal-oxide-semiconductor field effect transistor (MOSFET) Technology has emerged as the dominant technology used to design and fabricate semiconductor devices. [2]

2.1.1 MOSFET background

MOS-transistors are the building blocks of numerous logic, memory, and digital signal processing circuits. The MOSFET is a four terminal device formed by a MOS capacitor and two junctions. Figure 2.1 schematically depicts a MOSFET. The conduction in the channel region between the two junctions is determined by the voltages applied to the gate, source, and drain terminals. When the drain to source voltage is small, conduction between the source and drain junctions is modulated by the gate voltage. The MOSFET type is distinguished by the carriers in the conduction channel. The N-channel MOSFET (NMOS) has an n-type channel and operates by the conduction of electrons. A P-channel

MOSFET (PMOS) has p-type channel which operates by the conduction of holes. Complimentary-MOS devices combine both NMOS and PMOS structures. [3]

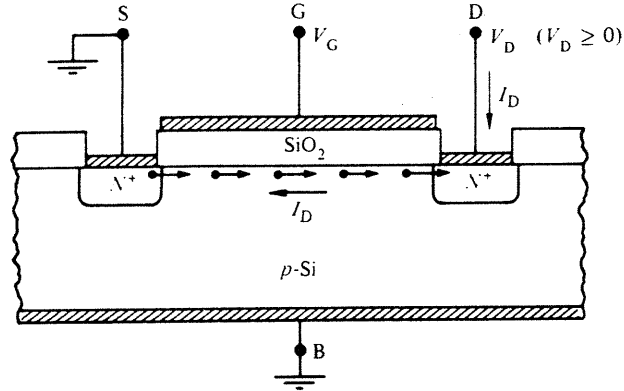


Figure 2.1 Schematic of an n-channel MOSFET under standard biasing conditions [4].

The threshold voltage (V_T) of a device is the voltage at which the MOS transistor channel begins to conduct current. This value is determined by the contributions from charge within the oxide layer, charge at the oxide-Si surface, and potential from the metal-semiconductor contact, given by the equation:

$$V_T = \Phi_{ms} + 2\Psi_f + \frac{Q}{C_{ox}} + \frac{Q_D}{C_{ox}} \quad \text{Equation 2.1}$$

where V_T is the threshold voltage (volts), Φ_{ms} is the gate-silicon work function difference (volts), Ψ_f is the electrostatic potential (volts), Q_{tot} is the total positive oxide charge, Q_D is the depletion region stored charge, and C_{ox} is the gate oxide capacitance (F/cm^2) [5].

MOS devices operate in one of two modes, enhancement or depletion, based on the Fermi level in the channel when no voltage is applied to the gate electrode. An enhancement mode device (normally off) requires a gate voltage greater than the threshold voltage (absolute value) for channel conduction. A depletion mode device (normally on) has channel conduction at zero gate voltage and requires a voltage greater than the threshold voltage (absolute value) to stop the source to drain current flow. Figure 2.2 shows the current-

voltage characteristics of the enhancement and depletion mode transistors for both NMOS and PMOS devices.

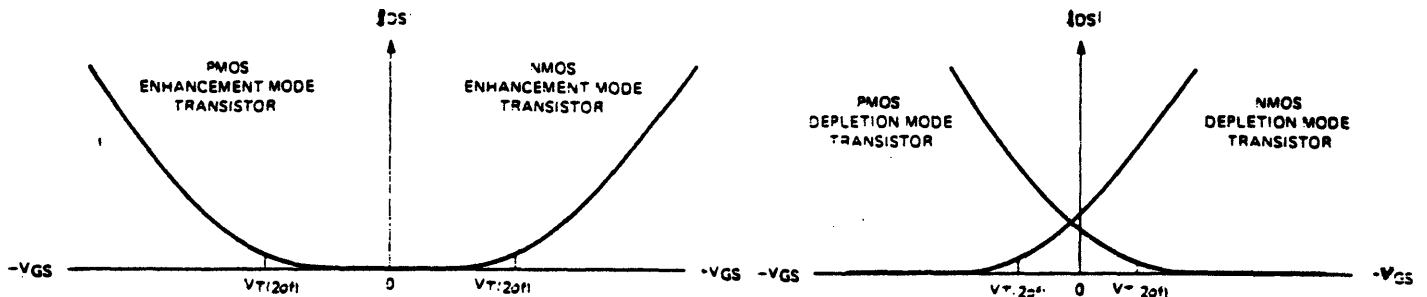


Figure 2.2 I_{DS} vs V_{GS} for PMOS and NMOS enhancement and depletion mode devices. [6]

The MOSFET offers scaling advantages and design flexibility. The Motorola PowerPC family of microprocessors is based on the complimentary metal-oxide-semiconductor field effect transistor (CMOS) process technology. CMOS devices offer many advantages over the NMOS devices including lower power dissipation, high speed, wide noise margin, and ease of circuit design. The twin well structure of the CMOS device offers additional advantages over other integrated circuit technologies including independent optimization of both the n-channel and p-channel transistors. [7]

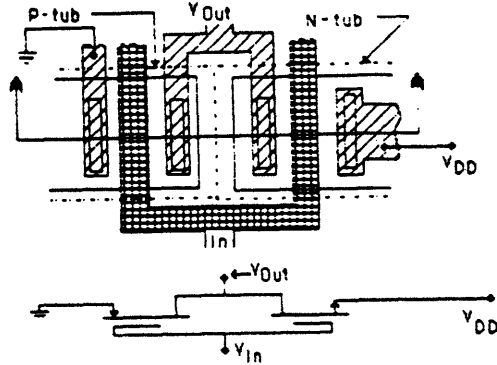
2.1.2 Semiconductor Fabrication

More than 100 process steps are required to fabricate semiconductor integrated circuits. The wafers must be lithographically patterned, doped, etched, and coated with various thin films. A basic process flow for CMOS fabrication is shown in Figure 2.3 [8]. The advances in device design and shrinking dimensions require controlled fabrication processes. Each of these processes must be carefully monitored and controlled to reliably produce products that meet stringent performance requirements.

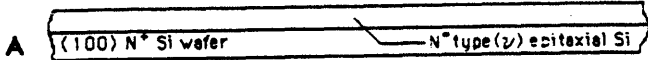
The fabrication of integrated circuits requires a process capable of uniform, controlled, reproducible introduction of dopant atoms into a semiconductor substrate. Diffusion and ion implantation are two techniques that are frequently used in device fabrication to incorporate dopant atoms into a substrate. In a diffusion process a

TWIN TUB, EPI CMOS PROCESS, $L=2\mu\text{m}$, LOCOS, POLYSILICON GATE.

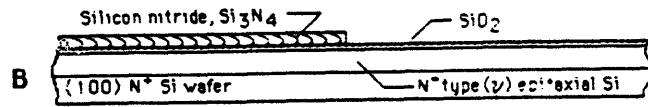
Starting Material: 100 - 150 mm (4-6 in) N-type (100) Silicon
 Resistivity range: 0.1 - 0.3 ohm-cm ($8E16 - 1.8E16$ atoms/cm³)



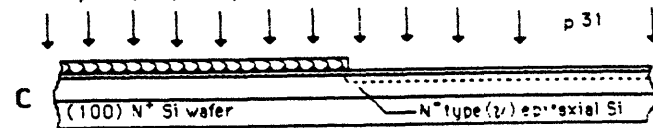
Deposit epi: 6-8 μm N-type Si, $1E13 - 1E14$ atoms/cm³.



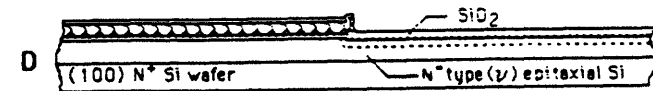
Stress-relief oxidation: 900-1050°C Dry O₂, 20-50 nm SiO₂.
 Deposit silicon nitride: 700-800°C LPCVD, 80-150 nm Si₃N₄.
 Mask 1: Field mask photolithography; Plasma etch nitride.



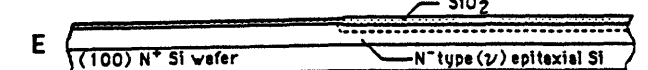
Implant phosphorus, N-tub. Implant is locally masked by nitride.



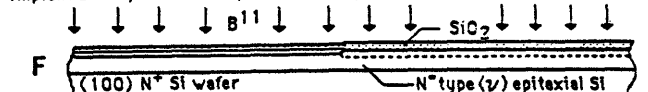
Short local oxidation in steam.



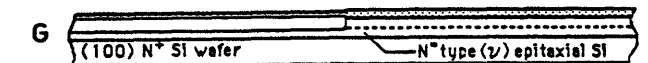
Remove oxide on nitride with dilute HF, then wet etch remove nitride.



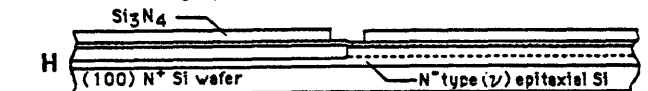
Implant Boron, P-well. Implant is locally masked by thicker oxide over N-well.



N-tub and P-tub Drive-in: 1100°-1150°C, 6-20 hours.
 Boron and phosphorus diffuse at about the same rate.



Deposit CVD Si₃N₄. Mask 2: Define regions of LOCOS field oxidation.



LOCOS field oxidation: 850-1050°C, steam, 5-16 hours, 0.6-1.0 μm SiO₂.



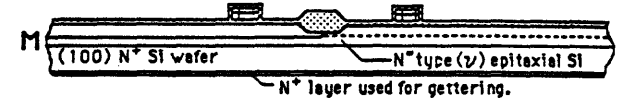
Remove oxide over nitride, wet etch nitride, remove stress-relief SiO₂.



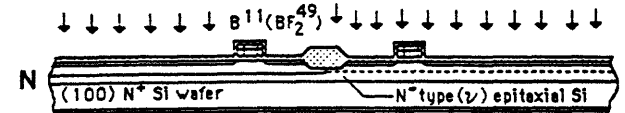
Grow gate oxide: 40-80 nm, dry O₂ (HCl), 900-1000°C or steam at lower temperatures. Measure critical gate oxide thickness.



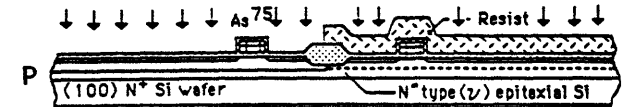
Deposit polysilicon, 0.4-0.6 μm ~ 625°C LPCVD. In-situ or post phosphorus doping of the polysilicon and back-side gettinger. Mask 3: Define poly gate. LPCVD deposit or grow oxide on polysilicon.



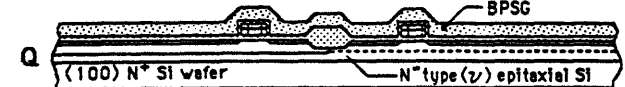
Implant boron or BF₂ over the whole surface to produce the source/drain of the PMOS device. Implant energy is low, to avoid boron penetration through gate oxide below polysilicon during drive-in.



Mask 4: Open NMOS device regions. Resist is mask to N⁺ implant. Implant arsenic to create Source/Drain for NMOS device.



Remove resist. Deposit LPCVD SiO₂, 0.4-0.8 μm , doped with ~ 4 wt% boron and ~ 5 wt% phosphorus. Reflow doped oxide and anneal implants, ~900°C.



Mask 5: Open contact windows. Remove resist.



Deposit barrier metal, then deposit 0.6-1.0 μm aluminum alloy by E-beam or sputtering. Mask 6: Etch aluminum and etch barrier metal. Then remove resist.

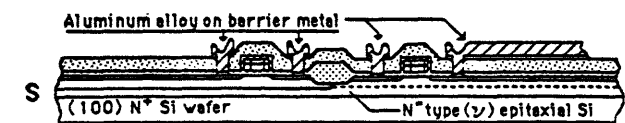


Figure 2.3 Basic process flow for CMOS device fabrication [8].

semiconductor wafer is heated in a quartz-tube furnace. The dopant ions are transported to the wafer by a carrier gas and incorporated in the surface. At sufficiently high temperatures (~900-1000°C for a Si substrate) the dopant atoms will diffuse from the surface of the substrate into the interior region. In this process dopant control depends on the uniformity of gas flow and surface conditions of the wafer. The flux of dopant atoms impinging the surface of the wafer must be uniform and the surface must be free of contaminants. Because these conditions are difficult to achieve reproducibly as required in a production environment, the second technique, ion implantation, is the technology of choice for uniform, controlled doping of semiconductors. [9]

Ion implantation has become an essential production process for manufacturing MOS, CMOS, BiCMOS, Bipolar, and GaAs process based solid state devices [10]. MOS transistors consist of p-n junctions which are formed by introducing electrically active impurities into a substrate in a controlled manner. Modern semiconductor devices may contain millions of transistors which must all be properly doped in order for the device to be functional. Ion implantation technology provides the capability for controlled doping of device structures, selection of dopant species, and spatial location of the implant within the device. Advances in device fabrication technologies have increasingly adopted and implemented ion implantation processes. The flexibility and compatibility of ion implantation with other fabrication processes enables rapid implementation of changes and advancing technology.

2.2 Ion Implantation Process Theory Background

The ion implantation process introduces a precise amount of dopants into a substrate using a beam of energetic ions which is scanned across the surface of the target wafer. The depth at which the ions penetrate into the substrate depends on the energy and mass of the dopant ion, the target mass, and the beam direction with respect to the crystallographic axes or planes of the target. In semiconductor processing the energy of the

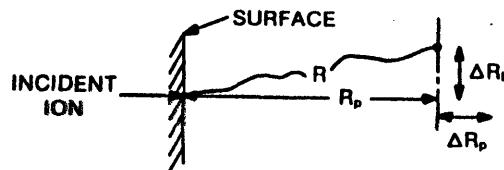


Figure 2.4 Schematic of the range R , projected range R_p , ΔR_p and ΔR_l [11].

dopant ions typically ranges from 3 to 250 keV for a singly charged specie. Advanced applications may utilize double or triple charged species with energies up to 750keV on a medium current implanter and 1MeV on a high energy implanter. Boron, phosphorus, and arsenic, are common dopant species with atomic masses of 11, 31, and 75, respectively. The total distance the ion travels, the range R, and the distance in the direction of incidence, the projected range R_p, are depicted in Figure 2.4. The ΔR_p and ΔR_l are defined as the perpendicular and lateral straggle [12]. The range can be approximated by the equation

$$R(\text{\AA}) = \frac{60E(\text{keV})}{g} \frac{M_2}{Z_2} \frac{M_1 + M_2}{M_1} \frac{(Z_1^{2/3} + Z_2^{2/3})^{1/2}}{Z_1} \quad \text{Equation 2.2}$$

where E is the energy, g is the target density, M is the atomic mass, Z is the atomic number, and the subscripts 1 and 2 refer to the incident ion and the target respectively [13]. The projected range is approximated by the equation [14]

$$R_p = R \left(1 + \frac{M_2}{3M_1}\right)^{-1} \quad \text{Equation 2.3}$$

and the ΔR_p is given by

$$\Delta R_p = \frac{2R_p \sqrt{M_1 M_2}}{3(M_1 + M_2)} \quad \text{Equation 2.4}$$

The implanted ion concentration as a function of depth in the substrate is approximated by a Gaussian relationship

$$n(x) = N_{\max} \exp[-(x - R_p)^2 / 2\Delta R_p^2] \quad \text{Equation 2.5}$$

where n is the concentration of ions, x is the depth, and N_{max} is the concentration at x=R_p [15]. If Φ is the total dose or flux of ions hitting the surface, then

$$N_{\max} = \frac{\Phi}{\sqrt{2\pi}\Delta R_p} = \frac{0.4\Phi}{\Delta R_p} \quad \text{Equation 2.6}$$

[16]. Other approximations have been developed to model the skewness of the concentration distributions due to ion size and backscattering effects. Figure 2.5 illustrates how a four-moment approach with a Pearson IV solution closely models actual concentration profiles.

In the implantation process, the bombarding ions collide with target nuclei and

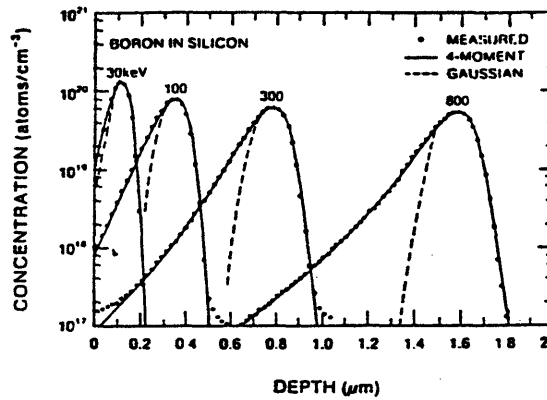


Figure 2.5 Boron implantation atom distributions for measured data, Pearson IV and Gaussian distributions [17].

interact with target electrons, losing kinetic energy as they penetrate a target. Ions entering the target transfer a large amount of kinetic energy, displacing the target atoms from lattice sites and damaging the crystal. Light ions such as Boron lose more energy via electronic interaction, resulting in fewer collision cascades. Heavier ions such as As or Sb induce more lattice damage because they lose most of their energy via nuclear collisions. Both heavy and light ions can form amorphous regions in the crystal if a large number of ions are implanted. Figure 2.6 illustrates the disorder produced by a light ion, heavy ion, and a beam of ions.

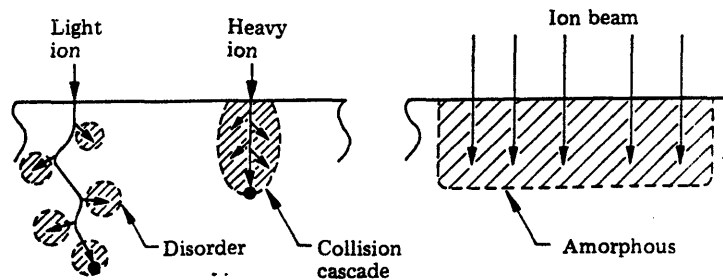
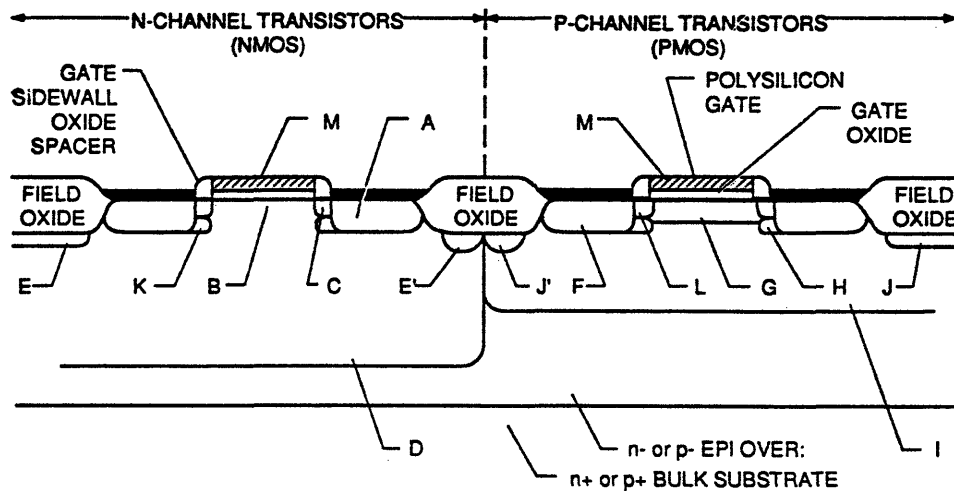


Figure 2.6 Disorder produced by light ion, heavy ion, and beam of ions forming an amorphous region [18].

Implanted ions must be incorporated into the semiconductor crystal lattice, occupying substitutional lattice sites, to be electrically active. The damaged regions that contain carrier traps and recombination centers must also be repaired to reduce the concentration of electrically degrading defects. Lattice repair and electrical activation can be accomplished by thermal annealing. Thermal annealing of Si can be achieved at temperatures ranging from 900-1000°C in approximately 30 minutes in a conventional furnace or 30 seconds in a rapid thermal process. The electrical sheet conductance of a semiconductor increases as crystal order is restored. [19]

2.3 Applications in CMOS Processing Technology

The growth of CMOS technology has increased the need for ion implantation applications. The standard CMOS device requires 7-9 implants. BiCMOS devices can utilize 15-17 implants while specialized circuits can employ more than 20 implants. Figure 2.7 illustrates the areas implanted in a standard CMOS process.



Implanted Regions and their Functions:

- A = NMOS source/drain; basic transistor structure.
- B = NMOS channel threshold voltage adjust; sets n-channel V_t (or V_p).
- C = NMOS LDD; hot carrier suppression.
- D = p-well ("tub") structure; contains NMOS transistors.
- E = p-type "channel stop" for p-well; intra-well (E) and inter-well (E') field isolation.
- F = PMOS source/drain; basic transistor structure.
- G = PMOS buried-channel threshold voltage adjust; sets p-channel V_t (or V_p).
- H = PMOS "punchthrough" suppression.
- I = n-well ("tub") structure; contains PMOS transistors.
- J = n-type "channel stop" for n-well; intra-well (J) and inter-well (J') field isolation.
- K = NMOS "punchthrough" suppression.
- L = PMOS LDD; hot carrier suppression.
- M = polysilicon gate doping (typically n+); improves conductance.

Figure 2.7 Regions implanted in a standard CMOS process [20].

Ion implantation is used to create wells, field channels, source areas, drain areas, voltage threshold adjustments (V_T adjusts), and source/drain extensions. Medium current implanters are utilized for the lower energy, lower dose implants. The higher dose and higher ion energy implants such as the source/drain implants require a high current implanter. New trends in CMOS design will soon require ultra high energy implanters (MeV) for retrograde well formation and device isolation improvements. Low energy implanters (plasma ion immersion implanters) are also being developed for shallow implant applications. [21]

One of the first applications of ion implantation in MOS processing was the well implant. Wells isolate the transistor and act as the transistor's back gate. Typical implants use B^+ or P^+ ions, 100-200keV energy, and $2-8 \times 10^{12} / \text{cm}^2$ doses [22]. The dopant concentration in the well near the surface directly affects the electrical performance characteristics of the transistor such as the threshold voltage, speed, and inter-device leakage currents. In modern CMOS technology, both n- and p-type wells are independently tailored to optimize the performance of both transistor types. The well implants are usually followed by a long, high temperature drive-in diffusion process to produce a deep junction structure.

Ion implantation is used to adjust the threshold voltage to optimize device performance. The dopant ions are implanted through a gate or sacrificial oxide into the underlying silicon. The change in V_T can be approximated by

$$\Delta V_T = \frac{qD}{C_{ox}} \quad \text{Equation 2.7}$$

where q is the elementary charge (Coulombs), D is the implanted dose (ions/ cm^2), and C_{ox} is the gate oxide capacitance (F/cm^2) [23]. Donor dopants will yield a negative V_T shift while acceptor dopants such as boron will increase V_T . The V_T of n-channel devices becomes positive with high doping concentrations and large gate oxide thicknesses. The voltage threshold implant requires precise adjustment of the dopant concentration under the gate oxide in the device channel. Ion implantation is the only process that can provide the required control over the dose, doping profile, and spatial uniformity. Threshold voltage adjust implants incorporate B^+ , P^+ , As^+ , or BF_2^+ ions at 20-150keV energies and 4×10^{11} - $6 \times 10^{12} / \text{cm}^2$ doses [24].

Field isolation implants increase the well doping near the well surface, preventing inadvertent inversion at the well surface and guarding against leakage currents. B^+ or P^+ , 40-150 keV, 5×10^{12} - 5×10^{13} dose, implants are used for intra- and inter-well isolation.

The dopant ions are implanted through the field oxide. Boron prevents leakage between the devices in the p-well while phosphorus suppresses leakage in the n-well. This implant process, found in all MOS fabrication processes, allows maximum CMOS circuit layout packing density. [25]

Source and drain implants form highly doped regions (10^{21} - $10^{22}/\text{cm}^3$) which act as a source and sink for carriers traveling across the device channel. N-type source and drain regions are typically formed with As^+ implants at energies ranging between 40-80keV, $2\text{-}6 \times 10^{15}/\text{cm}^2$ dose. P-type regions are implanted with BF_2^+ , 25-100 keV, $2\text{-}6 \times 10^{15}/\text{cm}^2$ dose or B^+ , 5-40keV, $2\text{-}6 \times 10^{15}/\text{cm}^2$ dose. Shallow junction formations required by CMOS devices employ additional Si or Ge implants to create an amorphous layer to control channeling effects. Lightly doped drain (LDD) implants are employed to reduce the hot carrier effect from the electric fields produced by the high concentration gradient between the source/drain and channel regions. Also called graded drain or tip implants, LDDs provide a gradual lateral dopant concentration which is essential for submicron transistors. [26]

CMOS processes use punchthrough suppression implants for both n- and p-type devices to prevent the drain depletion region from expanding into the lightly doped channel when the device is in operation. Punchthrough behavior can short channels and increase subthreshold leakage currents. B^+ , 40-100keV, $1\text{-}8 \times 10^{12}/\text{cm}^2$, implants are used for channel transistors. P^+ , 80-150 keV, $1\text{-}8 \times 10^{12}/\text{cm}^2$, implants are used for p-channel devices. The dopant is implanted below the active channel next to the source and drain regions. [27]

2.4 Process Requirements and Issues

The complexity of advanced VLSI device designs require precisely controlled doses, uniformity, minimal contamination, and energy and specie purity of the ion beam. The quality of the ion implant often times affects the device yield and reliability. Errors in dose or energy, contamination, or excessive wafer charging or heating can result in device performance degradation or even failure [28].

Variations in the dose across a wafer often results in unwanted variations in device performance, yield, and reliability. Non-uniform implants can be caused by several factors including electrostatic or mechanical scanning failures, fluctuations in beam size, and beam current drop-outs. Process monitors must be employed to detect dose variations before product wafers are affected. The data from the process monitors is usually recorded and

analyzed using a statistical process control (SPC) system. If the process is stable, the SPC system can be used to monitor, optimize, and control the process. This subject is discussed in the Appendix.

Contamination is a critical implant process issue when manufacturing devices with sub-micron geometries. Particulate contamination on the surface of the wafer during a processing step can cause defects in the structure of a device, leading to electrical failure including shorted or open circuits. In an implanter, particles are generated from moving mechanical parts and process residues such as photoresist or condensed ion source material. Figure 2.8 illustrates a particle on a wafer surface blocking an implant. The particle may even be a source for elemental contamination if atoms diffuse into the device during subsequent annealing or diffusion steps. The resulting partial implant or elemental contamination can lead to device failure [30]. Particulates in the beamline can interfere with the transport of the ions, adversely affecting the uniformity and repeatability of the implant process. Because the implant process is used many times in the fabrication of a device, the particulates generated by the implanter must be minimized.

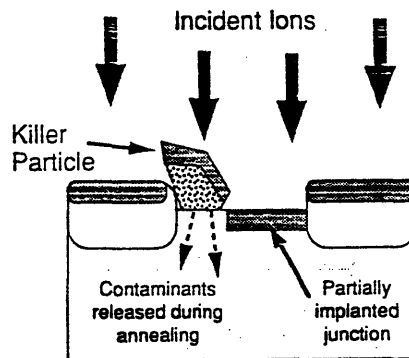


Figure 2.8 Particulate contamination blocking an implant and serving as an elemental contamination source [29].

Elemental contamination from implant processes that has been sputtered, implanted, or diffused into the silicon wafer can have detrimental effects on device yield and performance. The effects on the material properties depend on the type of contamination. Fast diffusing metals such as Cr, Fe, and Ni, form traps which act as recombination/generation centers, resulting in reduced minority carrier lifetimes, higher leakage currents, or device malfunctions. On the surface of the wafer these elements can form silicides during annealing steps which degrade the integrity of gate oxides in MOS

and CMOS devices. Aluminum contamination implanted in the silicon can shift threshold voltages. Na and K contamination in oxides can also contribute to threshold shifts and can even cause device malfunctions. The mobility of sodium ions in the device can cause the V_T to shift with time. The defect may not be detected at the factory and the shifting V_T can cause the device to fail during operation out in the field. [31]

Contamination is not limited to elemental contamination resulting from sputtered material in the beamline or particulate contamination. An ion implantation system must be designed to also control energy and specie purity of the ions implanted into the wafer. Neutral atoms, off-energy component ion, and disassociation products must be eliminated for proper dopant profiles and accurate dosimetry.

2.5 Metrology

Process characterization equipment is critical in monitoring controlling the ion implantation process in a production environment. Secondary Ion Mass Spectroscopy, Transmission Electron Microscopy, and Spreading Resistance Profiling are some of the methods used to determine the dopant specie, dose, depth profiles, and amount of energy and mass contamination in ion implanted wafers. Since these techniques are destructive, expensive, and time consuming, they can not be used as an effective daily or shiftly qualification measurement technique in production. Alternative electrical and optical methods provide the ability to quickly monitor the dopant dose and dopant uniformity across an implanted wafer. The Therma-wave and Four point probe (sheet resistance) are two techniques employed in production environments for measuring and tracking the dopant concentration and uniformity. Commercial probe systems offer a rapid method of collecting, analyzing, and presenting the data from dose monitor wafers. Both techniques measure a series of points across the entire surface of the wafer. The within wafer dose uniformity is represented by the standard deviation of the measurements made on a single wafer. The dose repeatability is determined by the standard deviation of the mean wafer measurements (each wafer represents an individual beam set-ups). These two metrology techniques will be briefly discussed in the following section. [32]

Laser scanners are used in implant metrology to monitor particulate contamination contributed during the implant process. Laser surface scanning inspection systems utilize photomultiplier tubes to detect scattered light from particles on bare silicon or oxide covered wafers. The particle performance is characterized by the delta particle count which is

determined by the difference of particle count measurements made before and after the process. [33]

2.5.1 Therma-wave Thermprobe Theory

Therma-wave Ion Implant Metrology is a widely used technique. Based on the optical-thermal response of the implanted material, it is the only non-destructive technique that can measure ion implantation on product wafers. The Therma-Probe TP-420 uses a 1 μm spot size so measurements can be made on actual product geometries. The measured thermawave signal is proportional to the amount of crystalline damage due to the implant. This technique is used to characterize low dose implant uniformity (1×10^{11} - $1 \times 10^{15}/\text{cm}^2$) across a wafer and run to run repeatability.

The thermawave technique utilizes the thermally dependent optical properties of a material. Variations in the sample temperature due to the thermal waves and thermal features are mirrored by modulations in the reflectance of the material. The thermawave signal is proportional to the change in reflectance as a function of temperature and electron plasma density. As the amount of crystalline damage increases, so does the value of the thermawave signal. The modulated reflectance is probed by a laser which is focused on the same spot on the sample surface as the heat generating pump laser. Figure 2.9 illustrates the optical measurement system. Time-variant heating generates thermal waves in a material. A low power laser beam focused to a 1 micron diameter spot increases the

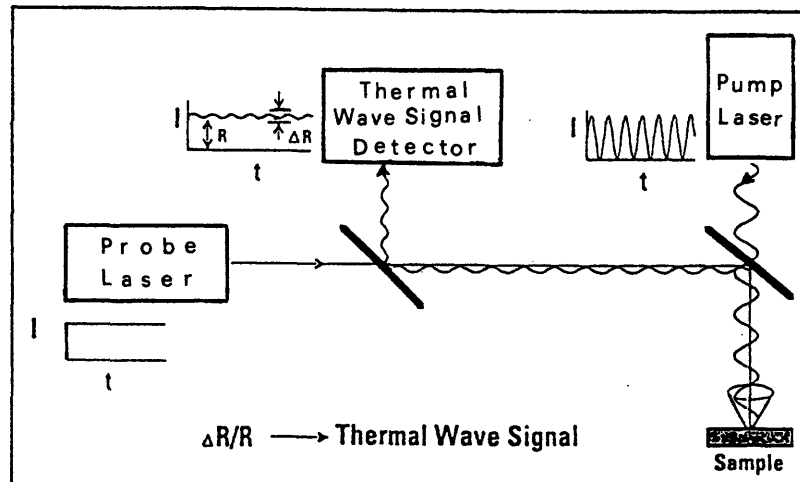


Figure 2.9 Thermaprobe optical system [35].

temperature in the illuminated area by 10°C (in silicon). Modulating the laser beam at a high frequency will create the periodic heating of the material needed to induce thermal waves and electron plasma waves which diffuse and propagate into the substrate material. In silicon the waves can propagate 2-5 micrometers below the surface before they are critically damped. Local variations in composition, impurity concentration, and lattice perturbations, exhibit variations in thermal properties (conductivity and volume specific heat) relative to the homogeneous bulk material and affect the propagation of the thermal waves. These thermal features located within 2-5 microns of the sample surface are detected by their interaction with the laser pump-generated thermal waves. Although this measurement varies with species, dose, energy, beam current, beam density, screen oxide conditions, temperature during the measurement, and crystalline orientation of the wafer, it can be used effectively to monitor the performance of an implanter for low doses. [34]

2.5.2 Four Point Probe

The four-point probe is commonly used to measure sheet resistance of implanted wafers. The sheet resistance measurement, R_s , used for characterizing thin layers is given by the equation:

$$R_s = \frac{\rho}{t} \quad \text{Equation 2.8}$$

where ρ is the resistivity and t is the thickness of the layer [36]. The resistivity of a semiconducting material is dependent on the carrier concentration. The effects of dopant concentration on resistivity are illustrated in Figure 2.10.

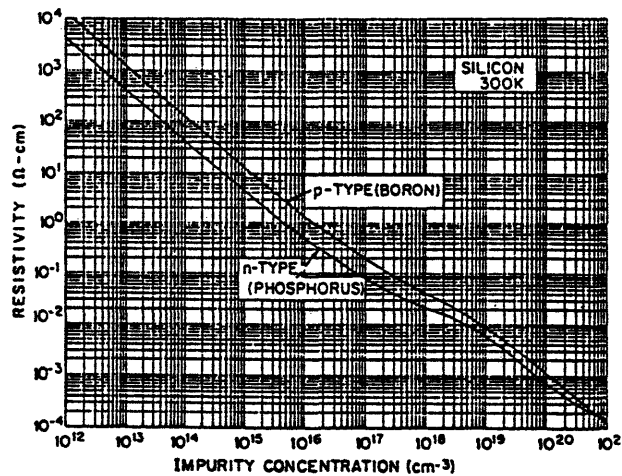


Figure 2.10 Resistivity vs. dopant concentration [37].

Four point probes use probe head assemblies that contain four pins arranged in either a linear or square array as depicted in Figure 2.11. The probe tip spacing is represented by S . The sheet resistance is measured by supplying a current (I) through two pins and measuring the voltage drop (V) between the other two pins. The sheet resistance is then given by

$$R_s = k\left(\frac{V}{I}\right) \quad \text{Equation 2.9}$$

where k is a correction factor which compensates for geometric effects such as probe tip spacing and array configuration. For configurations with equal probe tip spacing, the k values for linear and square arrays are 4.532 and 9.064, respectively. Sheet resistance measurements of semiconductor wafers are useful in production environments for monitoring ion implant processes and equipment because of their accuracy, repeatability, and low equipment cost.[38]

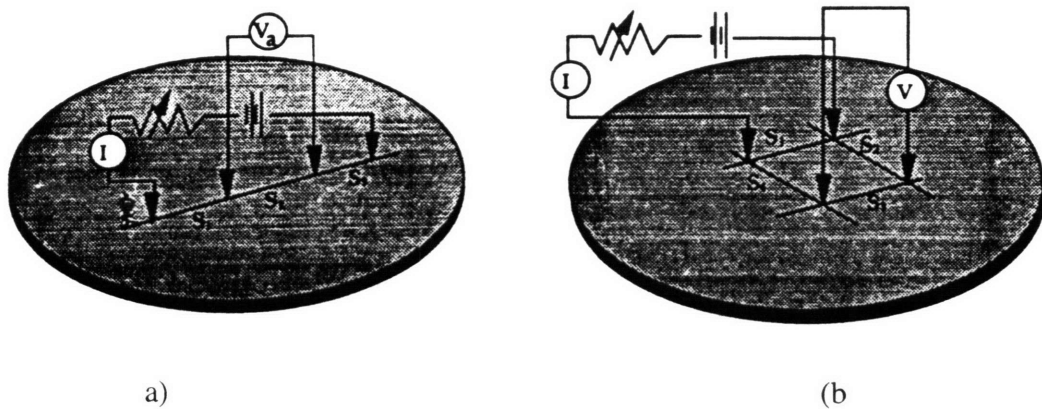


Figure 2.11 (a) Linear and (b)square configurations of probe head assemblies [39].

Chapter 3

Ion Implantation Systems

3.1 General Systems Overview

Ion implantation systems are complex, integrated systems which are capable of generating a beam of energetic ions from a gas or solid source and transporting the ions to a substrate at a specific energy and beam current. The major components of an implanter include an ion source, extraction mechanism, mass analyzing system, accelerating column, beam scanning system, and end station (target chamber and cassette loading area). The ions are produced in the ion source housing assembly, extracted from the source, transported down the beamline through mass analyzer magnets, acceleration columns, and focusing elements, and directed towards the target substrate. The source area, beamline and target chamber are usually under a high vacuum system (on the order of 1×10^{-7} Torr) to minimize scatter and neutralization of the ions in the beam as they are transported from the source to the target. Implanters are classified according to the operating beam current intensities or ion energies. Low current implanter have beam currents on the order of 0.1mA, medium current ~1mA, high current ~10mA. High energy implanters can generate 1MeV ion beams and low energy implanters can generate ion beams with <10 keV energies.[40]

The ion source assembly is a critical component in an industrial ion implanter. The performance of an ion source directly impacts the process quality and production efficiency of the implanter. The process quality is measured by the ion current stability, available current, and the production efficiency is measured by utilization and throughput. The development of the hot cathode ion source technology enabled the commercial use of high current and medium current implanters. The two most commonly used source designs in the

semiconductor production environment are the enhanced Bernas Source and the Freeman Source. The arc chamber configurations are illustrated in Figures 3.1.

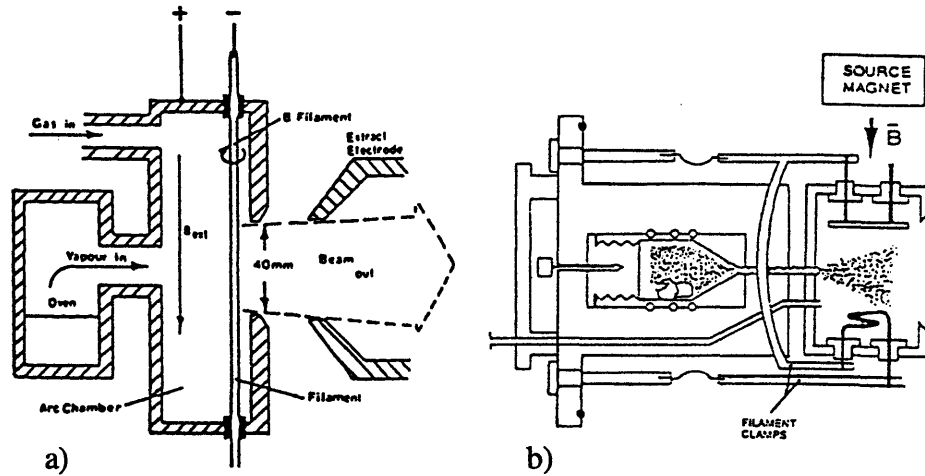


Figure 3.1 (a) Freeman source and (b) Bernas source configurations [41].

The species to be implanted is ionized by electrons which are thermionically emitted from a tungsten filament in the arc chamber. Thermionically emitted electrons are accelerated through a potential between the filament and arc chamber (arc voltage). The energetic electrons collide with neutral atoms in a vapor containing the desired dopant molecules, creating the ion plasma. A magnetic field enhances the ionization efficiency of the electrons by altering the trajectories into a spiral shape. Important process parameters include the vaporizer temperature (if the source material is a solid), source pressure, filament current, arc voltage, arc current, and source magnetic field.

The ion beam is extracted from the plasma in the arc chamber through an aperture with an accelerating voltage. The ion beam contains different atomic and molecular ion species which are separated out in a mass analyzing magnet. Electric and magnetic fields along the beam transport system focus the diverging beam and increase (or decrease) the ion energy. To reduce the risk of dose error and an undesirable dopant profile caused by disassociation products of multiply charged ion species produced during beam transport, systems employ energy filters. Most commercial systems have high voltage source, magnet, and beamline regions. The high voltages used for the plasma generation and beam extraction mechanism, make the the implanter highly susceptible to arcing problems. Excessive arcing can cause internal damage to the implanter hardware and electronics.

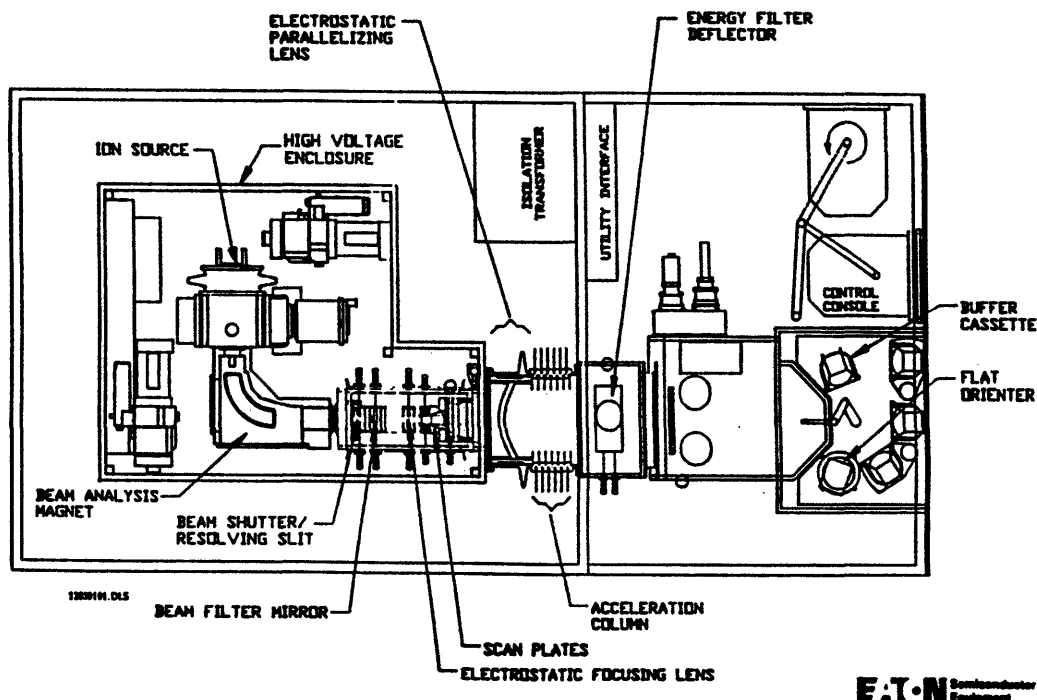
The beam is scanned across the surface of the target wafer either electrostatically and/or mechanically . A current integrator is utilized to measure the dose by keeping track of the total current collected. Systems may also contain elements to minimize wafer charging

and cooling. These issues are more problematic for high current implanters. The energy from the bombarding ions is dissipated as heat. Excessive heating of the wafers can damage the photoresist or affect the damage induced to the crystal lattice. Gas cooling platen designs have been implemented to reduce the wafer temperature during the implant. Wafer charging can cause uniformity problems or even electrical breakdowns in insulating layers used during processing (oxides, nitrides, and photoresist). To minimize the detrimental effects of wafer charging on device yields, systems employ secondary electron showers. Wafer charging has not been a problem for serial mode medium current implanters because of the lower beam currents and high beam scan speeds. [42,43]

3.2 Eaton NV-8200P Medium Current Ion Implantation System

The Eaton NV-8200P is a serial process medium current ion implanter. Configured with an enhanced Bernas source and a 4 bottle gas box, it can implant 3 species with energies ranging from 3-750 keV and beam currents from 4 μ A to 4mA. The implanter is equipped with two energy filters to eliminate off-energy contamination. It also employs quadrupole focussing elements and a parallelizing lens to focus the ion beam. The hybrid electrostatic/mechanical scanning system is used to raster the beam to scan the wafer, providing a uniform implant. A schematic of the implanter layout is shown in Figure 3.2.

Figure 3.2 Schematic of the NV-8200P System [44].



The Eaton NV-8200P is a fully-automated, parallel scanning medium current ion implanter. The SN825 machine was configured to process eight inch diameter wafers in a continuous serial processing mode. The implanter was designed to minimize contamination in both the beamline and wafer handling environments. For maximum beam purity the system employs two energy filters, a reflective energy filter (REF) and an angular energy filter (AEF). The wafers are handled in a class 1 laminar environment with a 3-axis robot arm. The wafers are aligned with respect to the wafer notch, moved through a vacuum load lock, and transferred to the implanting platen in the process chamber. The platen assembly is capable of tilting the wafer 0°-60°, initially orienting the wafer 0°- 360°, and repositioning the wafer during the implant process.

The NV-8200P source housing assembly contains a Bernas source, arc chamber, and materials feed system. Source materials are fed into the source chamber from a gas handling system or from one of the two vaporizer crucibles. The gas box has the capacity for 1 inert gas bottle (argon) and 3 toxic gas bottles. The ion beam is then extracted from the source area by the "accel-decel" lens/suppressor extraction system. The extraction electrode manipulator assembly can be adjusted on three axes to optimize the beam conditions. The extraction gap (distance of the electrode to the source chamber) and alignment settings of the electrode (tilt angle and side axis position) can be automatically or manually adjusted. The NV-8200P mass analysis system consists of a 90° radially indexed dipole magnet that has 250 millimeter bending radius and a mass*energy product of 3130 AMU *keV. This allows ions species with an AMU of 78 or lower to be extracted using the maximum extraction potential (40kV). The source area and magnet are cooled with self-contained, recirculating deionized water (deionized water is used to prevent arcs from striking and damaging water lines).

The beam shutter assembly, located after the magnet, consists of a resolving aperture as well as an electrostatic scanner which deflects the beam in the horizontal direction. The beam shutter is used to interrupt the beam between implants. The post analysis beam filter removes disassociation product ions (for multiply charged species) which have passed through the analyzer magnet using an electrostatic mirror to repel and eject off-energy ions from the beam(which are considered as contaminants) and allow the desired multiply charged specie to pass.

The beam is electrostatically scanned in the horizontal (x-axis) direction into a fan shaped pattern. The system's beam parallelizing lens (p-lens) then corrects the angle of the beam into a ribbon shaped pattern. The beam is then accelerated or decelerated to the desired energy in a uniform gradient acceleration column. A set of quadrapole lenses optically

focuses and centers the beam. The post acceleration energy filter is an electrostatic deflector and energy resolving aperture. The beam is deflected 15° to minimize neutral and off-energy contaminants just before the beam strikes the wafer in the target chamber. The automatic energy tracking feature of the NV-8200P controls the energy filter, focusing elements, p-lens, accel/decel, and extraction voltages to achieve the desired final beam energy. The p-lens voltage is 1.7 times the extraction voltage and the accel/decel voltage is set so that the sum of the extraction, p-lens, and accel/decel voltages yields the desired total beam energy.

The wafer handling system consists of a rotary transfer robot arm with a vacuum pick that contacts only the back side of the wafer. In the vacuum load lock the transfer arm which loads the wafers the the implant platen also only contacts the back side. The robot performs load and unload operations simultaneously to optimize the throughput. The wafer platen tilts and rotates the wafer to desired positions programmed in the recipe to prevent channeling. During the implant, a scanning arm moves the wafer platen in a linear path perpendicular to the electrostatic scan direction so the beam can scan the wafer in the vertical (y-axis) direction.

The NV-8200P dosimetry system performs pre-implant scan uniformity measurements, pre-implant spot size measurements, pre-implant beam divergence measurements, and dose sampling. A beam profiler assembly is mechanically scanned across the target region to determine the uniformity of the electrostatic x-scan. During an implant a faraday cup continually samples the beam for dosimetry calculations. A dose cup calibration is performed before implanting the first wafer of a batch to ensure accurate dosimetry.

The NV-8200P source area, beamline, and endstation must all be in a high vacuum environment to minimize contamination and ensure efficient beam transport. The vacuum system includes turbomolecular pumps for the source area and beamline and CTI Cryo-Torr Eight cryogenic pumps for the post acceleration energy filter and process chamber. The system can be monitored from the operator interface and the cryogenic pumps can be automatically regenerated.

The control system consists of a workstation linked to a bus controller. The bus controller is connected to device interfaces which drive the sensors and actuators used by the control system. The implanter has the capability to automatically set-up the ion beam and process wafers. Recipes programmed in the software specify all of the desired implant parameters (species, energy, beam current, dose, target orientation, etc.) for the auto set-up.

[45]

Chapter 4

Source Inspection

4.1 Test Description and Procedure

Source inspection testing of process equipment is common practice in the semiconductor industry. Since the equipment suppliers often receive more than 50% of the multimillion dollar cost of a tool when it is shipped to the customer, the tool is tested by the customer at the vendor site before it is shipped. Equipment problems or defects are generally easier to fix at the factory than at the customer site because of the availability of parts and system experts. The purpose of the source inspection of MOS-13's first NV-8200P (serial number (SN) 825) was to verify that the equipment was functional and built according to Motorola specifications.

The source inspection testing for the SN825 implanter consisted of two visits to the manufacturing factory. The first visit, the 50% source inspection, was a one day review of the progress of the machine build when the tool was approximately 50% complete. The equipment configuration was checked and any issues which would have delayed the final inspection or delivery were addressed. The second factory visit, the final source inspection, involved a review of the Eaton final test results, a five day process performance battery of tests, and a final equipment configuration inspection.

The Eaton final acceptance test is a standard test performed on all implanters manufactured at the factory. This test verifies that the implanter meets Eaton vacuum system specifications, boron beam current specifications, phosphorus beam current specifications, arsenic beam current specifications, beam stability tests, dose uniformity specifications, and wafer cycling requirements. The test is completed by the Eaton final

test engineer responsible for the customer acceptance before the customer final source inspection test.

The Motorola source inspection process performance test is a battery of beam performance tests, auto-set-up sequences, process performance, and wafer handling/cycling tests designed by the Motorola process engineer. The SN825 test was designed by Alan Laulusa and Navjot Chhabra. The maximum beam currents for different dopant species and energies were tested by manually tuning ion beams to specified currents, documenting the beam parameters at the desired current (the software enabled screen printouts). Two hour beam stability tests for unscanned beams of different species and energies were scheduled. A chart recorder was attached to the flag assembly to record the unscanned beam current as a function of time. The beam could not "glitch" more than 10 times in a two-hour period. A glitch is a sudden beam drop-out or spike in the beam current due to an arc or other variation in the source area that is greater than ten percent of the beam current. Figure 4.1 shows a glitch in an otherwise stable beam.

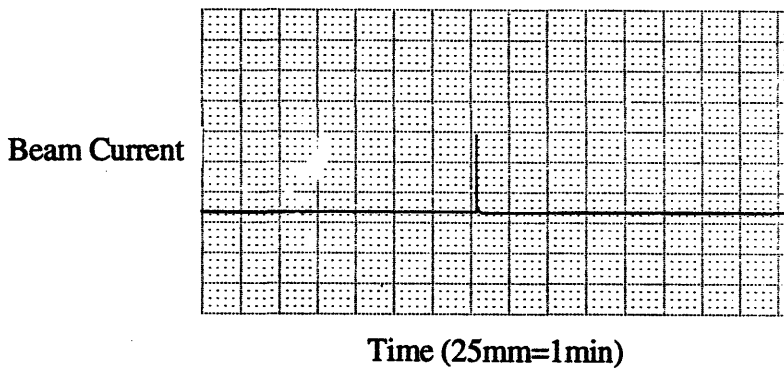


Figure 4.1 Beam current glitch.

The beam auto-tune capability and process performance of the implanter were tested using a number of process recipes which tested the full range of energies and doses for As⁺, B⁺, BF₂⁺ and P⁺ implants. A full cassette of 25 wafers was implanted for each recipe. At least one test wafer was monitored for dose uniformity per batch and the rest of the cassette was filled with recycled dummy implant wafers. The wafer to wafer dose uniformity was determined by measuring the dose from 2 wafers implanted with one beam

set-up. The test wafers were measured using the APRDL TP-420 (Therma-wave). Particle contamination was not measured during the source inspection.

The wafer handling throughput and reliability were tested when the implanter was not running beam tests. The implanter was put in a cycling mode and wafers were repeatedly cycled through all the positions, cassette-notch aligner-load lock-chuck-load lock-buffer-cassette, without being implanted. The response to misloaded wafers was also tested during the implant tests. Wafers from boats were intentionally cross-slotted or removed from cassette slots to check the software alarms and wafer mapping.

The final source inspection test for the second MOS-13 implanter, SN842, was revised to specifically focus on dose repeatability, recipe auto-tune set-up times, and wafer handling. Two recipes, an arsenic high dose monitor and a boron low dose monitor, were repeated 25 times in an alternating order to ensure separate beam set-ups. The auto-tune capability was tested by running set-up sequences of 10 different recipes without implanting wafers. The wafer handling was tested using all 3 cassette positions and partially filled cassette with cross-slotted wafers and numerous missing wafers. A fast implant recipe set-up was used to cycle the wafers through the implant chamber. Slot integrity and wafer mapping were monitored.

4.2 Results

The SN825 implanter passed the final source inspection after two weeks of testing, completing 77 beam performance and implant process tests. Several mechanical failures caused major delays in the testing. All of the manually tuned arsenic, boron, and phosphorus maximum beam current and stability tests were passed. The within wafer dose variation (dose uniformity) of the implanted wafers was less than 0.5% (TW) for most of the recipes with the exception of 60, 65, and 70 keV, B⁺ and As⁺ implants which had variations ranging from 1-2%. The P⁺⁺⁺ implant could not be completed due to an unstable beam. The wafer to wafer uniformity within a batch (recipe set-up) was acceptable. The set-up times for changing recipes within the same species solid or gas was under 10 minutes. Gas to solid source material specie changeover set-up times ranged from 56-86 minutes, while solid to gas specie changeover set-up times were 21-64 minutes. The wafer handling system responded well to missing wafers and cross-slotted wafers and successfully completed cycling tests without dropping or breaking wafers.

The second MOS-13 medium current ion implanter SN842 passed both the 50% source inspection and final inspection in December 1995. The maximum beam current and stability tests were completed and passed by the Eaton final test engineer before the final

inspection. The SN842 dose uniformity and the run to run repeatability for the dose monitors improved during the course of the testing to acceptable values. The autotune set-up times were on target for the gas to solid changeovers and adequate for the within species beam set-ups. The wafer handling system had trouble correctly mapping and handling missing and cross-slotted wafers.

4.3 Discussion

The 50% inspection of SN825 was completed and passed by Terry Breeden. The final source inspection of SN825 was plagued with several catastrophies that caused the inspection to last two weeks. Vacuum leaks, a wafer handling mishap, broken wire, vibrating scanning arm, and grinding beam profiler mechanism, were some of the equipment problems encountered during the process testing. The maximum beam current testing and stability tests were time consuming especially for the solid source material species. The challenging beam stability tests at maximum beam currents were difficult to pass. All of the tests were failed at least once due to major arcs, beam drop-outs, or system leaks. The time of the beam stability testing was decreased to 1 hour (not more than 5 glitches). The implant recipes were not all taught and tested before our arrival so each recipe required a manual tuning which took at least an hour in addition the automatic set-up which needed to be tested. A newer version of software was used for tests 49-78 to improve the auto-tune set-up time and capability. This decreased the number of manual assists during the beam tuning and increased the frequency of recipe set-up times under 10 minutes.

The wafer handling problems encountered during the SN842 source inspection were linked to both sensor problems on the robot arm as well as software issues. A recalibration of the macobot (robot arm) improved some of the mapping problems. The system errored and could not recover when wafers were missing at the top of a cassette (split lot mode). This problem needs to be addressed in the next software version.

4.4 Conclusion

The source inspection testing results gave a good preview of the overall equipment performance. After two weeks of testing and successful completion of the final source inspection, the ion implanter SN825 was conditionally accepted and approved to be shipped to Motorola. The conditional terms were based on the rectification of all outstanding issues during the inspection, including a functional 3 color lighttower and

audible alarm, improved auto-tune capability with a software upgrade (to be released after the inspection), and other specified parts which were not located during the inspection.

The revised final source inspection test for SN842 proved to be more efficient method of identifying problems with the top equipment issues of dose uniformity, repeatability, and wafer handling. A dose uniformity problem was detected early enough so that the problem could be fixed and the implanter could be accepted on schedule. The extensive format of the SN825 source inspection may be reserved for the 2.0 qualification if the resources (time and test wafers) are available. The SN842 implanter was conditionally accepted and approved for shipment to Motorola.

Chapter 5

Testing for the RFW Qualification

5.1 Test Procedure

The first phase of the equipment qualification procedure after the FAB installation is the RFW Qualification. Successful completion of the RFW qualification tests signifies that the equipment is ready to run product wafers. This battery of tests, which fingerprints the baseline performance of the system and verifies that the process performance matches that of the Motorola Advanced Product Research & Development Lab (APRDL) implanter, is conducted after the supplier has completed all system calibrations, minimal beam and process performance testing, and system safety tests (electrical interlocks, emergency shut-off, and radiation tests).

The three RFW qualification tests targeted the top two implant manufacturing process issue categories, dosimetry and contamination. The first test assessed the dose uniformity and repeatability using two dose monitor recipes. The second test determined the dose accuracy by a process recipe matching procedure with an implanter in the APRDL facility which ran a comparable process. The third test analyzed the surface and sub-surface elemental contamination resulting from the ion implantation process. Particulate contamination due to the implanter was determined during the first two tests.

The dose uniformity and repeatability test was conducted using two dose monitor recipes, a high dose recipe and a low dose recipe. Each recipe was repeated 15 times and the recipes were alternated to ensure an independent beam set-up for each implant. An argon purge of the system was run between each of the test set-ups to minimize interspecie contamination. A full cassette of two new test wafers and 23 dummy wafers were

implanted for each recipe set-up. The test wafers were scanned for a pre-implant particle count ($\geq 0.3 \mu\text{m}$ size) using the APRDL Tencor 6200 particle scanner, implanted on the SN825 medium current implanter with the appropriate recipe, and then scanned again for the post-implant particle count. Thermawave measurements for both the high and low dose monitor test wafers were then conducted on the APRDL Thermaprobe TP-420. The implanted wafers from the high dose monitor runs were annealed in the MOS-13 HTE rapid thermal annealing furnace for approximately 30 seconds at 950°C and then probed for the sheet resistance measurements on the MOS-13 Prometrix RS55/tc four point probe.

The process matching test was conducted using a series of arsenic, boron, and phosphorus process recipes. One test wafer was implanted per recipe per set-up. The recipes were set-up in an alternating order to ensure independent beam set-ups. Particle counts were measured before and after the implant process. The recipes were repeated 15 times except for Process 4 and Process 6 (due to time and resource restrictions). Thermawave measurements were completed after the post-implant particle count.

The elemental contamination test was conducted using an As^+ , 250 keV, $5 \times 10^{15} / \text{cm}^2$ dose, 2.5mA beam current, recipe. Two p-type test wafers were dipped in a dilute HF solution to strip the native oxide and remove any surface contamination. One of the wafers was implanted with the arsenic recipe. The unimplanted wafer was used as a control sample for the SIMS analysis. The samples were analyzed using TXRF to detect surface contamination and SIMS for sub-surface elemental contamination. The MOS-13 TREX 610, using a tungsten rotating anode source was used for the TXRF analysis. Samples were measured in the center and at the edge of the wafer. The MOS-13 Cameca IMS-3f was used for the SIMS analysis.

5.2 Results

The results from the dose uniformity and repeatability test indicate that the dose uniformity averages for the high dose monitor and the low dose monitor were on the order of 0.7% (RS55) and 0.4% (TW) respectively. The run to run repeatability for both the high dose and low dose monitors was greater than 1%. The process matching was characterized by the $\% \Delta$ which is the percent difference between the SN825 average value for a particular recipe and the APRDL average value for the same recipe. Most of the process recipes matched within 1 percent of the APRDL values. The high dose monitor was off by 4.4%. The results are summarized in Table 5.1. The particle contamination was initially higher than desired but fell within acceptable limits during the latter part of the testing.

The TXRF data and the SIMS data showed a significant amount of elemental contamination. The surface concentration of Fe exceeded the allowable amount. All other concentrations of metallics were within acceptable limits. An aluminum profile was also discovered from the SIMS analysis suggesting that there was a significant amount of energetic aluminum contamination. Na and Al were present as both surface and implanted contamination. The Al concentration peak was located at a depth of 0.32 μm and the Na peak was 0.45 μm below the surface.

Table 5.1 Process Recipe Matching Data

Recipe	Metrology Tool	% delta
High dose	RS55/tc (ohms/sq)	4.40
Low dose	TP-420 (TW units)	0.86
Process 1	TP-420	0.90
Process 2	TP-420	0.72
Process 3	TP-420	1.40
Process 4	TP-420	0.97
Process 5	TP-420	0.09
Process 6	TP-420	0.17

5.3 Discussion

The implanter has the capability to adjust the dose of the individual recipes by a dose trim factor. All of the recipes were initially run without a dose trim adjustments. After eight runs of each of the dose monitor recipes and 2 runs of each of the matching recipes the results indicated that the implanter was underdosing the wafers by approximately 5% on all recipes. The dose trim factor was adjusted immediately to conserve time and resources. Fifteen additional runs of each dose monitor was run for a sufficient sample size. The results reflected in Table 5.1 only include the results after the trim was implemented.

A statistical comparison of the MOS-13 and APRDL data sets could not be done for the process matching because the APRDL implanter was very limited (one data point on some process recipes). Ideally the implants should have been run simultaneously on both implanters and measured at the same time on the same metrology tool. A lack of personnel, time, and resources, prevented the testing procedure to be completed in this manner.

The high particle counts at the beginning of the testing were attributed to the implanter's "settling in" period. The machine had been disassembled in a class 10,000

environment, transported to Motorola, and reassembled. Particles in the system, especially those emanating from the motion of mechanical parts, can usually be cleaned out by running the system and cycling wafers. Dummy wafers were implanted with Arsenic to help clean the beamline and cycled to exercise and clean the mechanical mechanisms (robot wafer loading arm, load lock, transfer arm, and chuck).

The initial results of the elemental contamination test did not pass the RFW qualification requirements. The depth of the Al peak suggests that the energy of the Al ions being implanted into the wafer was approximately 220 keV. The energy of the contamination indicates that the contamination originated before the p-lens (after the mass analyzer), was accelerated down the beamline, and implanted into the wafer. The elemental contamination test was repeated to verify the results. The follow-up test examined the As⁺, 250 keV, and $5 \times 10^{15}/\text{cm}^2$ dose implant and two process recipe implants. The results verified that the sub-surface contamination was present for the high energy, high dose, As recipe but no sub-surface Al or Na contamination was found in the process recipe implants. An unacceptable amount of surface Fe contamination was observed on the As implanted wafer but not on the other two process wafers. The data suggests that contaminants are being sputtered from Al beamline parts and deposited during high energy-high beam current implants. The Fe contamination is attributed to the fact that the Al alloy used for the beamline parts contains Fe. Replacement of the Al parts susceptible to sputtering during beam transport should resolve the elemental contamination issue. Since no detectable amounts of contamination were introduced during the normal process operating conditions, the high energy-high beam current recipe elemental contamination test was waived for the RFW qualification.

5.4 Conclusion

The RFW qualification evaluated the short term process performance of the SN825 medium current ion implanter. Based on the test results, the SN825 implanter passed the RFW qualification. The baseline performance of the dosimetry and contamination levels were documented. The dose uniformity, repeatability, and accuracy (matching), were adequate to start processing the first production qualification wafers. Production specification limits of the dosimetry parameters need to be analyzed based on device parametric data from the first production qualification lots.

Chapter 6

Testing for the 2.0 Qualification

6.1 Test Description and Procedure

The complete equipment-process evaluation at the Motorola site is called the 2.0 Qualification Testing. The purpose of the testing is to assess the capability of the equipment to function in a production environment. The system must operate in a fully automatic mode, providing a quality process which conforms to all beam performance, dosimetry, wafer throughput, contamination, and system performance and reliability requirements as specified in the Equipment Purchase Agreement (EPA). The performance requirements are outlined in Section 2.0 of the EPA. Any approved discrepancies that the supplier, Eaton Corporation, had with the requirements were documented in the addendum. The battery of tests for the 2.0 testing have been designed with these minimum requirements as a guide. Successful completion of the 2.0 qualification signifies that the equipment meets the Motorola minimum standards and is ready to start the warranty period. The warranty agreement is based on the fulfillment of the process performance requirements as well as the system reliability performance (uptime, mean time to failure, etc.). Months can be added or subtracted from the warranty period based on process and reliability performance. Failure to meet all of the 2.0 requirements results in added months of warranty service and can become very costly for the equipment supplier.

The tests for the 2.0 qualification were designed to prove that the Eaton NV-8200P medium current implanters, SN825 and SN842, were capable of running a stable, repeatable process in an automatic mode. The methodology and results of testing the first

system, SN825, are presented in the following sections. The second implanter was scheduled to be tested in March 1996.

The beam performance capability of the implanter was evaluated with a series of tests which assessed the beam current production, beam stability, and the beam energy stability. The beam currents and beam energies for the species to be tested are summarized in Table 6.1. Beam current stability tests were conducted for the specie-energy-beam current combinations marked in bold print. Less than 5 glitches (as specified in the source inspection testing) were allowed per hour.

Table 6.1 Maximum Beam Current Specifications

Energy (keV)	Beam Current (μA)						
	B11 ⁺	B ⁺⁺	BF ₂ ⁺	P31 ⁺	P ⁺⁺	P ⁺⁺⁺	As75 ⁺
3	350			260			150
10	1000			1000			500
250	2000		1500	3500			3500
500		150			1000		
750						250	

The testing of the NV-8200P medium current ion implanter included an evaluation of the system dosimetry. The dose accuracy, energy accuracy, uniformity, and run to run (set-up to set-up) repeatability, were assessed. The system was tested three times daily (by different operators) using the daily qualification recipe. One test wafer was scanned for particles, implanted, scanned for particles, annealed using the 950ANNEA recipe, and measured on the four point probe. The support equipment included the Tencor 6420 particle scanner, HTE furnace, and Prometrix RS55/tc. An additional qualification recipe was monitored on a less frequent basis, usually after any type of maintenance work on the system.

The particle defect contamination tests were conducted for all implanted wafers used in the dosimetry tests. The scanner was programmed to detect 0.2 μm sized particles and larger.

The interspecie contamination test was conducted using a series of 6 implants alternating between BF⁺ (amu 30) and P⁺(amu 31). One test wafer was implanted per recipe set-up. The recipes were automatically set-up without an argon purge between the

different species. Gas mass spectrums were recorded before and after each implant. The six wafers were then analyzed for boron and phosphorus profiles using SIMS.

6.2 Results

The implanter passed the beam performance tests. The four point probe and particle contamination measurements for the daily qualification recipe were tracked on trend charts (x-bar -s and c type attribute charts, respectively) in the MOS-13 computerized SPC system. The process matching data for the daily qual recipe was statistically analyzed using JMP software. The t-test analysis indicated that the data from the two implanters, MOS-13 and APRDL, was statistically different and did not match. Due to the confidential proprietary nature of the information, the exact results and graphical representation of the data cannot be shown. The average dose uniformity, repeatability, and APRDL dose matching, for the qualification recipe did not meet the 2.0 qualification requirements. The particulate contamination was acceptable as well as the auto recipe set-up times. The interspecie results did not meet the 2.0 specification. Boron was detected in the phosphorus implants. The SIMS analysis of the boron recipe test wafers did not indicate the expected boron profile. An unexpected phosphorus profile was detected in these wafers.

6.3 Discussion

The within wafer dose uniformity improved since the RFW qualification. On a few occasions the uniformity met the 2.0 requirement but the overall average did not meet the specification. Several experiments and analyses of process parameters were conducted to identify key factors affecting the uniformity. The electrode axis settings, beam shape, beam profile symmetry, empirical correction factors, and scan amplitude setting were the parameters investigated for the dosimetry problems. No direct correlations could be drawn between the electrode axis settings and the uniformity. Anomalies in the side axis setting which seemed to affect the beam profile symmetry and beam shape were linked to dose monitors with high within wafer non-uniformity problems but the results could not be reproduced. The beam shape and profile symmetry seemed to also affect the efficiency of the predicted non-uniformity correction factor derivation and dose. The empirical correction factors (ECFs) allow the process engineer the ability to adjust the beam scanning speeds across the wafer in eight zones. These values were experimentally determined by measuring a diameter scan of an implanted wafer and calculating the values for the eight zones. The results did not show a significant improvement in the wafer uniformity. Implementing the default empirical correction factors yielded better results. The ECFs did

not work for implants using beam currents less than 100 μ A. No correlation between the scan amplitude setting which controls how far the beam travels in the horizontal direction and the dose uniformity was found.

The run to run repeatability also improved from the RFW testing, but the EPA requirement was not met. Periods of run to run set-up stability were often offset by step function shifts in the dose measurements. This is usually a problem when different operators have to manually set-up recipes. Since the tests were run in an automatic set-up mode as they would be in a production environment, the variation of beam parameters due to different operators was eliminated. The beam shape and symmetry seemed to affect the dose but data proving this in a controlled experiment was difficult to produce. The scan amplitude setting had an affect on the dose. The scan amplitude had to be sufficiently large to completely overscan the faraday dose cup and ensure proper claculation of the dose. Incomplete scanning resulted in dose variations, degrading the process repeatability. Dose repeatability was one of the most challenging issues to address because the implanter system is a dynamic system. The ion source changes as it it used and the set-up parameters for the filament current, arc current, and beam optics (including the extraction electrode settings) vary with the source life. The recipe set-up data files, "histories," for a new source was dramatically different from a history saved from an older source. The dose uniformity and repeatability must therefore be desensitized to these factors. Eaton has proposed two hardware developments designed to improve dose repeatabililty which will be available later this year. Preliminary data shows improved performance of the parts but the effects on long term dose repeatability have not been proven.

The dose matching on the daily quailification recipe was difficult to achieve because the target (APRDL) was constantly moving. Most of the dosimetry work focused on stabilizing the process performance (of both systems) and then adjusting the process to the desired target based on parametric data and device performance. The dosimetry metrics did not exclude the variation of the metrology tools. Usually the implanter process performance is extracted from the total variation however, the 2.0 qualification requirements were stated in terms of direct readings from the metrology printouts.

The automatic set-up times improved dramatically during the course of the 2.0 testing. During the RFW qualification the average set-up time was 18 minutes with several manual tunes which was not acceptable for the 2.0 qualification. The auto set-up time is critical to running high volume production on a serial implanter because it decreases the process throughput. Each new version of software seemed to improve this function, finding a more efficient and optimal method of beam set-up. One of the auto set-up problems, especially for low current implants, was the beam profiling and correction factor

routine. Since the beam was profiled at a rate proportional to the beam current, lower beam current recipes took longer to profile and achieve the desired predicted non-uniformity value. The time to reach the predicted non-uniformity value also influenced by the accuracy of the calculated beam scanning correction factors. A symmetric initial beam profile improved the efficiency of calculating the correction factors. The recipe histories required some maintenance (manual re-tuning), especially after source changes in order to achieve a better overall average for the auto set-up time test. This will become a problem when processing high volumes of wafers requires frequent source changes and re-tuning of a hundred product recipes.

The wafer handling requirement is somewhat deceiving because it quotes a mechanical throughput at 190 wafers per hour. In a real production environment this throughput could never be realized because wafers need to be implanted and not merely cycled through all the positions. The Eaton final test engineer believed that operating at this speed would wear the mechanical robot parts without offering much of a gain on wafer throughput.

The surface and sub-surface elemental contamination data from the RFW qualification test does not meet the 2.0 requirement. The iron and aluminum contamination for high energy and high dose implants exceeded the maximum allowable amount. The aluminum contamination is believed to be sputtered from the surfaces which the ion beam comes into contact with from the source to the target. Most of the parts are made of aluminum. The iron contamination may be from the iron contained in the aluminum alloy used for all the parts in the beamline (scan plates, accel column, reflective energy filter, etc.). Eaton issued an engineering change order to modify the system, replacing several parts which are in direct contact with the ion beam with graphite or silicon coated aluminum parts. Preliminary results from two implanters at other sites indicate that the graphite and siliconized parts modification significantly reduces the amount of surface and energetic aluminum contamination. Due to the significant amount of time required for this modification and the aggressive manufacturing schedule, this could not be attempted until the second medium current implanter was installed and RFW qualified (March 1996). The elemental contamination test was repeated for the 2.0 qualification after the equipment modification was implemented. The modification was implemented in early February. The results showed an order of magnitude reduction in the amount of energetic aluminum. The carbon contamination from the new graphite parts remained at acceptable levels.

The interspecies contamination test was repeated with the P⁺ implants preceding the BF⁺ implants. Gas mass spectrums were measured before and after each implant. The SIMS analysis of the test wafers did not detect the expected boron profile in the BF⁺

implanted wafers. Trace amounts of boron (barely greater than the background level) were detected. Immediately after the specie gas switchover from phosphine to boron trifluoride, the spectrums showed peaks at AMU 29, and 30, and no peak at 31. There was a peak at 62 indicating that phosphorus was still in the source area. This suggests that the analyzer magnet and software detected the phosphorus peak first and tagged it as AMU "30" and then tagged the BF^+ peak as AMU 29. Since the recipe called for a specie with the AMU of 30, P^+ was implanted instead of BF^+ . The phosphorus implanted wafers had the correct specie and dose. Boron was also detected in the phosphorus wafers suggested a considerable amount of interspecie contamination. Eaton is revising the software so that it does not rename the amu peaks in the spectrum.

6.4 Conclusion

Based on the number of items that did not meet the EPA section 2.0 requirements, the Eaton NV-8200P medium current ion implanter SN825 failed the Motorola 2.0 qualification. The within wafer dose uniformity and run to run dose repeatability were improved during the testing but still did not meet the minimum requirements. Process matching to the APRDL implanter (dosimetry) was postponed until long term dose repeatability could be demonstrated on both machines. The implanter was incapable of passing the interspecie contamination test because of the method in which the software selected the dopant material. Many hours were invested in helping the implanter pass as many of the requirements as possible. Many hours were invested in understanding the system dynamics and their affects on the processing and subsequent device performance. Numerous equipment modifications to improve reliability and enable the system to meet 2.0 qualification requirements were implemented. Some of the 2.0 qualification shortcomings such as the energetic Al contamination did not stop production because they didn't affect the implants in the region of operation. This battery of tests successfully identified the areas that needed improvement. The results were communicated to the supplier, Eaton, and active efforts to improve the process performance of the 8200P have been initiated. The SN842 implanter already showed improvements at the source inspection. The SN825 implanter will not begin the warranty period until all of the requirements are met.

Chapter 7

Summary and Recommendations for Future Work

The qualification testing of the Eaton NV-8200P Medium Current Ion Implanter was conducted in a production environment. Because the system was still in its developmental stage, characterizing and qualifying the Eaton NV-8200P in a factory start-up environment proved to be a challenging task. The implanter failed to meet the minimum process requirements for uniformity, repeatability, interspecie contamination, and metals contamination. The 2.0 qualification was scheduled to be completed 23 days after the facilitization of the equipment at the Motorola site and the supplier start-up. The testing period was extended to allow for the implementation of equipment upgrades that would enable the system to meet the performance requirements. The qualification required a joint effort between myself and the Eaton engineers that designed the system to characterize the factors that affected the dose uniformity and run to run repeatability.

The implementation of hardware and software upgrades are necessary to meet the processing specifications of the 2.0 qualification. Specific modifications that need to be installed before further process characterization testing include a new extraction electrode assembly, graphite and siliconized beamline parts, arc chamber stability improvements, and the software version that addresses the analyzer magnet selection and labeling. Over 70 equipment modifications have been implemented in the SN825 implanter to improve the system reliability and process performance. Items to pursue that may improve process control are the in situ particle monitor that was supposed to be available in early 1996 and the SPC system that is currently employed in the high current machine. The SPC system would enable the process engineer to easily extract, analyze, and monitor data from all of the process beam parameters.

The device parametrics indicated that the device was tolerant of implant dose variations produced by SN825. Device performance analyses need to be completed in order to properly set targets and specification limits on the implant processes and determine if the daily qualification procedures are adequate. Once this is completed, the true process capability can be statistically evaluated. Device performance analyses are often complicated by the fact that other factors in the production process line also affect the parametric results. The initial process specification limits left little room for error in other processes, several of which may affect critical parametrics. An attempt was made to link variations in parametric data to variations in the dose monitor measurements. This preliminary analysis of the data did not yield conclusive results. These correlations need to be studied further to ensure accurate dose monitoring and process control procedures.

Motorola and Eaton learned a significant amount of information about the NV-8200P system from the implanter qualification testing. The information learned from the testing procedure of the first MOS-13 implanter enabled more efficient testing of the second NV-8200P, SN842. Although the implanter did not meet all of the 2.0 testing specifications, appreciable improvements in the system performance resulted from the joint effort. Improvements in the system reliability (measured by the uptime and mean time between service), auto-tune recipe set-up time, dose uniformity, and repeatability were made during the implanter qualification. This partner relationship must be continued in order to reach the qualification process performance goals and maintain the best medium current ion implantation process available in the industry.

Appendix

Statistical Process Control

Statistical process control (SPC) is a manufacturing strategy used by process engineers to monitor, optimize, and control processes. The output of a process is statistically analyzed and monitored to determine if a process is operating within the predicted range of natural variation. This method can be used to prevent misprocessing product if the process or related equipment problem is detected on a process monitor.

All processes have a natural variation, a random fluctuating pattern of results, centered about a mean measurement. A large number of data points usually has normal (Gaussian) distribution as shown in Figure A.1.

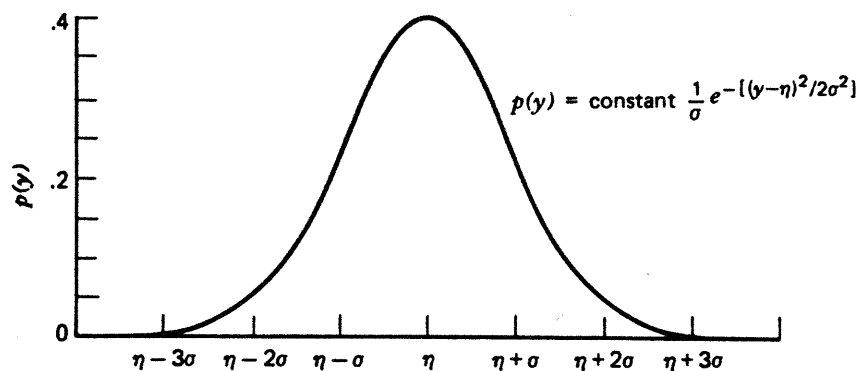


Figure A.1 The normal (Gaussian) distribution [46].

If the process is stable, this distribution is constant over time. The amount of variation (the spread) is characterized by the standard deviation, σ , the square root of the process variance, σ^2 , which is given by

$$\sigma^2 = \frac{\sum(y - \eta)^2}{N} \quad \text{Equation A.1}$$

where y is the measurement, η is the mean, and N is the number of samples measured [47]. A complete discussion of these statistical metrics can be found in *Statistics for Experimenters* by Box, Hunter, and J. Hunter (reference 46).

An SPC system employs control charts to visually represent changes that occur in a series of process measurements. Control charts are categorized as attribute and variables charts, depending on the type of data being collected. Attribute data is discrete data such as count or pass/fail data. Particle contamination data is typically displayed on a c-type attribute control chart. Variables data is continuous data such as film thickness or dose measurements. The different types of attribute and variable control charts are discussed in *Six Sigma Process Control: Guide to Standardized Process Control Practices*. The correct type of chart must be selected for the type of data collected otherwise the charts will not be an effective tool for process control. Control charts are trend charts with a centerline and control limits. Figure A.2 illustrates a typical control chart.

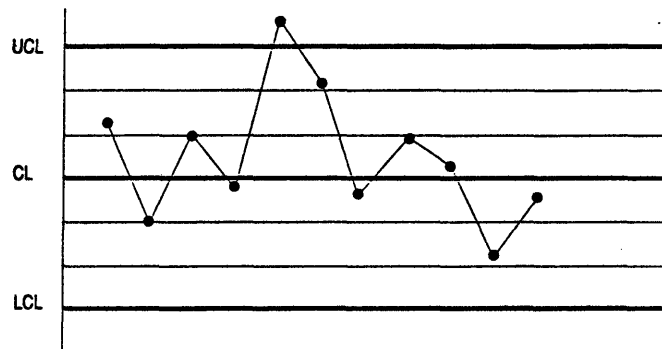


Figure A.2 Control chart. [48]

The statistical limits (control limits) of a process are conventionally set at 3 standard deviations (σ) above and below the mean of the process. Common characteristics of a stable process include, a random pattern of results showing no trends, constant mean, uniform variability over time, most points are near the centerline, and no points are outside the control limits. Control charts are analyzed for trends which may lead to an out of control process. Computerized systems often incorporate rules such as the WECO rules to determine if a process is in control. These rules are discussed in the *SPC Refresher Module* (reference 49) These Statistical quality control (SQC) charts are also used to

monitor processes. These charts show the data relative to product specification target values and the upper and lower specification limits are determined by product performance. [49]

Controlling a process is directly associated with controlling the equipment. For example, an equipment maintenance procedure for an ion implanter can sometimes be predicted by the dose variation of a daily dose monitor. A build up of photoresist due to outgassing from a large number of wafers can sometimes coat the dose measurement system, causing the implanter to overdose wafers. This is indicated by a shift in the process average to a lower sheet resistance value (increased dose). When the dose measurement falls below the process control limits the dose measurement parts must be cleaned. Other problems with scan mechanisms can also be detected by unusually high variations in dose uniformity across the wafer.

Other metrics which describe the process performance include the potential process capability index (C_p), process capability index (C_{pk}), and the instability index (St). The C_p and C_{pk} indices are used to determine how well a process conforms to process specifications. The C_p assumes that the process is centered on the target and is given by

$$C_p = (USL - LSL) / 6\sigma \quad \text{Equation A.1}$$

where USL is the upper spec limit, LSL is the lower spec limit, and s is the standard deviation. A smaller process spread (less variation) will yield a larger C_p value, indicating a better process. The C_{pk} is used when a process is not centered on the target and is calculated using the equation:

$$C_{pk} = (\text{Mean} - \text{Closer Spec Limit}) / 3\sigma \quad \text{Equation A.2}$$

The C_{pk} index is large when the mean is close to the target and the process spread is small. When the process is centered on the target, the C_p and the C_{pk} indices are equal. The instability index measures the fraction of points that are out of control. [50]

References

1. Rimini, Emanuele. Ion Implantation: Basics to Device Fabrication Kluwer Academic Publishers; Boston, 1995, p1.
2. Technology Associates, Semiconductor Technology Handbook. 1985 p1.5.
3. ibid p12.10-18.
4. Pierrret, Robert F. Modular Series on Solid State Devices Vol. IV Field Effect Devices 2nd Ed. Addison-Wesley; Reading, MA, 1990, p66.
5. San Angelo, D. Eaton Memorandum on GSD Low Dose Implants.
6. Technology Associates, p12.15.
7. Simonton, Robert and F. Sinclair. "Ion Implantation Applications in Process Technology" Handbook of Ion Implantation Technology. edited by J.F. Ziegler. Elsevier Science Publishers B.V.; New York, 1992, p273.
8. Technology Associates, p1.12-18.
9. Mayer, J.W. and S.S.Lau. Electronic Materials Science: For Integrated Circuits in Si and GaAs. Macmillan Publishing Company; New York, 1990, p183, 222.
10. Simonton and Sinclair, p272.
11. Murarka, S.P. and Martin Peckerar. Electronic Materials Science and Technology. Academic Press, Inc; Boston, 1985, p218.
12. ibid, p518-9.
13. ibid, p220.
14. ibid, p221.
15. ibid, p222.
16. ibid, p222.
17. ibid, p228.
18. Mayer and Lau, p235-6.
19. ibid p239.
20. Simonton and Sinclair, p277.
21. ibid, p284-351.
22. ibid, p278.
23. Rimini, p265.
24. Simonton and Sinclair, p276.
25. ibid, p280.
26. ibid, p282.
27. ibid, p283.
28. Current M.I. et al. "Process Control for Ion Implantation" Handbook of Ion Implantation Technology Ed. J.F. Ziegler. North-Holland; New York, 1992, p 648.
29. Smith, T.C. "Photoresist and Particulate Problems" Handbook of Ion Implantation Technology Ed. J.F. Ziegler. North-Holland; New York, 1992. p580.
30. ibid, p580.
31. Ryssel and I. Frey. "Contamination Problems In Ion Implantation" Handbook of Ion Implantation Technology Ed. J.F. Ziegler North-Holland; New York, 1992, p691.
32. Current, p651-3.
33. ibid, p651-3.
34. Thermo-wave ThermoProbe TP-420 Operation Manual
35. Rimini, 71.
36. Tencor Prometrix RS55/tc Operation Manual, pA2.
37. Rimini, 7.
38. Tencor Prometrix RS55/tc Operation Manual, pA7.
39. ibid, pA2-8.
40. Rimini, p33-34.

41. *ibid*, p37.
42. *ibid*, 35-66.
43. Eaton NV-8200P Technical Reference Training Manual Chapters 1,2, and 5.
44. Simonton , Robert Presentation In Situ Monitoring In The Eaton NV-8200P Medium Current Ion Implantation System, 1992.
45. Eaton NV-8200P Technical Reference Training Manual Chapters 1,2, and 5.
46. Box, Hunter, and J. Stuart Hunter. Statistics for Experimenters: An Introduction to Design, Data Analysis, and Model Building. Wiley and Sons; New York, 1978 p43.
47. *ibid*, p39.
48. Bedell and Huy Phan. Six Sigma Process Control: Guide to Standardized Process Control Practices. Motorola, Inc; Phoenix, 1993 p21.
49. Motorola SPC Refresher Module, MOS13, Aug 1995 p1-30.
50. Bedell and Phan. p30-33.